

# A Deep-Learning Framework to Predict the Dynamics of a Human-Driven Vehicle Based on the Road Geometry

Luca Paparusso, Stefano Melzi, *Member, IEEE*, and Francesco Braghin, *Member, IEEE*

**Abstract**—Many trajectory forecasting methods, implementing deterministic and stochastic models, have been presented in the last decade for automotive applications. In this work, a deep-learning framework is proposed to model and predict the evolution of the coupled driver-vehicle system dynamics. Particularly, we aim to describe how the road geometry affects the actions performed by the driver. Differently from other works, the problem is formulated in such a way that the user may specify the features of interest. Nonetheless, we propose a set of features that is commonly used for automotive control applications to practically show the functioning of the algorithm. To solve the prediction problem, a deep recurrent neural network based on Long Short-Term Memory autoencoders is designed. It fuses the information on the road geometry and the past driver-vehicle system dynamics to produce context-aware predictions. Also, the complexity of the neural network is constrained to favour its use in online control tasks. The efficacy of the proposed approach was verified in a case study centered on motion cueing algorithms, using a dataset collected during test sessions of a non-professional driver on a dynamic driving simulator. A 3D track with complex geometry was employed as driving environment to render the prediction task challenging. Finally, the robustness of the neural network to changes in the driver and track was investigated to set guidelines for future works.

**Index Terms**—Trajectory forecasting, motion cueing, recurrent neural network, driver-vehicle system, road geometry

## I. INTRODUCTION

THE field of control systems has considerably benefited from the advances in deep learning obtained in the last decade. The reason is to be found in the excellent results achieved by deep-learning algorithms in modelling complex dynamical systems [1], [2]. Particularly, modern control applications as autonomous driving and robot navigation, which deal with a dynamic and varied environment, need to manage more information to properly model the whole dynamics of the scene, including the behaviour of other autonomous agents or the interactions between humans and machines. As a consequence, the resulting dynamics becomes rather articulated, and in many cases it is even arduous to interpret the underlying physics that governs the system evolution. Under these conditions, data-driven models, especially deep-learning frameworks, have been demonstrated to embody a viable and efficient alternative to classical first-principle models.

This work has been submitted to the IEEE for possible publication. Copyright may be transferred without notice, after which this version may no longer be accessible.

The authors are with the Department of Mechanical Engineering, Politecnico di Milano, Milan, Italy [luca.paparusso@polimi.it](mailto:luca.paparusso@polimi.it)

Trajectory forecasting algorithms constitute one of the most important applications of deep learning in the area of control systems. They generate predictions on the future behaviour of the agents in the control scenario, which can be used to enhance the promptness and performance of the controlled system. In [3], Long Short-Term Memory (LSTM) neural networks are used to predict the acceleration distributions of cars on highway, modelling in-lane motion only. A probabilistic deep neural network is designed in [4] to predict distributions of vehicles trajectories in a roundabout, i.e. in-plane positions at any time instant, assuming that each vehicle can be modelled through its in-plane position, heading and longitudinal velocity. In [5], [6], motion recognition and trajectory forecasting algorithms are applied to human-robot collaboration tasks, in which collision avoidance and safety guarantees constitute a strict requirement. Convolutional Neural Networks (CNN) are employed in [7] to predict the motion of pedestrians for autonomous driving applications. Finally, a different approach to trajectory forecasting for control tasks, presented in [8], consists in producing state-space equation models as outputs of the network, to describe the coupled dynamics linking the ego-robot with the other agents in the scene. This methodology allows to consider the effects of the control actions taken by the ego-robot on the other agents and generate control-aware predictions. As a further advantage of this method, the generated model, following the state-space form, can be directly employed for planning and control tasks.

In this work, we focus on a problem that has been the core of automotive research for half a century, that is modelling and forecasting the dynamics of the coupled system constituted by a human driver and the vehicle that he/she drives [9], [10]. The dynamics of the vehicle, in terms of response of its constitutive elements to known driving inputs, e.g. throttle, was widely investigated in the past [11]–[13]. However, modelling the decision-making process of a human driver, namely the control actions that he/she executes considering environment, still represents an open research field. Unlike autonomous navigation systems, a human driver shows a varied, stochastic and, most of the times, non-optimal behaviour. Moreover, each driver has a personal driving style, which is strictly related to his/her own experience.

Many works have tried to emulate human drivers using control systems, e.g. [14], with simplified models for the vehicle dynamics. These architectures allow to accurately describe the behaviour of professional drivers on track, whose aim is to minimise the lap time, but it could be difficult or even

impossible to tune them so as to replicate a non-professional driver. To take into account the complex coupling effects between the driver and vehicle systems, and to capture the human nature of the driver, data-driven approaches may be employed to model and forecast the evolution of the whole system. Also, the high modelling performance of these methods allows to investigate how the geometry of the road influences the future decisions of the driver, which is one of the key contributions introduced in this work. A 3D track is then selected as driving environment to introduce higher variability into the resulting motion trajectories, which makes the prediction problem particularly challenging.

We propose a deep-learning framework, based on LSTM autoencoders, to predict the future state trajectories of the driver-vehicle system. The framework is designed to be general purpose, so that the user can specify the part of the dynamics that he is interested to model and predict. Without losing generality, to show the performance of the forecasting algorithm in practice we select a set of features that can be measured/estimated and used for common control applications. Aiming to reproduce the driving behaviour of a human, the network fuses information on the realised past with the road geometry that the driver is about to travel, to generate context-aware predictions of the desired features for a predefined number of future time steps.

We introduce a parametric loss function to train the neural network. It allows to control the relative importance between forecasting errors on primary features, i.e. the ones of interest, and on secondary features, i.e. the auxiliary ones employed to help the network learning the dynamics of the system. Using constrained optimisation, the loss function hyperparameter and the number of trainable parameters of the network are tuned to achieve a suitable trade-off between forecasting performance and computational time during the test phase. The latter is in fact fundamental in online implementations for control purposes.

The control applications that can benefit from the proposed problem formulation and prediction strategy are several, from the design of Advanced Driver-Assistance Systems (ADAS) to human behaviour imitation. In this work, we validate our approach applying it to a case study regarding motion cueing algorithms. An experimental campaign is conducted on a dynamic driving simulator to collect the dataset, train and validate the neural network. Finally, to demonstrate the efficacy of the proposed framework in understanding the relationship between the road geometry and the actions taken by the driver, the trained deep neural network is applied to new data, generated by simulations with a different driver and a different track.

The rest of this paper is organised as follows. The prediction problem is formulated in Sec. II. In Sec. III, the proposed deep-learning architecture to solve the prediction problem is presented. The application of our method to the case study, centered on motion cueing algorithms, and the corresponding results are reported in Sec. IV; in the same section, the dataset preparation and the hyperparameters tuning procedure are extensively described. In Sec. V, we further investigate the generalisation properties of the proposed method, by testing

it on data obtained with a different driver and a different track. Finally, the conclusions of this work and potential future studies are presented in Sec. VI.

## II. PROBLEM FORMULATION

The goal of this work is the design of a deep-learning framework to predict the evolution of a set of user-specified quantities related to the dynamics of the coupled driver-vehicle system, which moves on a track with complex geometry. Therefore, the formulation of the prediction problem shall be based on the emulation of the decision-making process of a human driver. At any time instant, a driver is aware of the vehicle state and his/her previous driving actions, which carry information about the recent past context that he/she has operated in. However, the past only does not provide a complete picture to characterise the resulting motion. In fact, drivers are highly conditioned by the road geometry that they see ahead, and act accordingly. Therefore, the intuition at the basis of the proposed formulation is to include information on the road geometry into the prediction model, so as to highlight the dependency between driving actions and environment properties.

The previous statements are now formalised in mathematical notation. Let us consider the current time step  $k \in \mathbb{N}$ . Given the 3D geometry of the track, that is the spatial location of the centerline and the road margins; given matrix  $X_{(k-t^P:k)}$  describing the values assumed by  $n \in \mathbb{N}$  vehicle features monitored in the last  $t^P + 1$  time steps, where  $t^P \in \mathbb{N}$ ; the objective is to predict matrix  $X_{(k+1:k+t^F)}$ , describing the values assumed by  $q \in \mathbb{N}$  vehicle features in the future  $t^F$  time steps, where  $t^F \in \mathbb{N}$ ,  $t^F \geq 1$ . The  $q$  features are a subset of the  $n$  features monitored in the past, thus  $q \leq n$ . The matrices  $X_{(k-t^P:k)}$  and  $X_{(k+1:k+t^F)}$  are defined as

$$X_{(k-t^P:k)} := \begin{bmatrix} x_{k-t^P}^1 & x_{k-t^P}^2 & \dots & x_{k-t^P}^n \\ x_{k-t^P+1}^1 & x_{k-t^P+1}^2 & \dots & x_{k-t^P+1}^n \\ \dots & \dots & \dots & \dots \\ x_k^1 & x_k^2 & \dots & x_k^n \end{bmatrix}, \quad (1)$$

$$X_{(k+1:k+t^F)} := \begin{bmatrix} x_{k+1}^1 & x_{k+1}^2 & \dots & x_{k+1}^q \\ x_{k+2}^1 & x_{k+2}^2 & \dots & x_{k+2}^q \\ \dots & \dots & \dots & \dots \\ x_{k+t^F}^1 & x_{k+t^F}^2 & \dots & x_{k+t^F}^q \end{bmatrix},$$

where  $x_i^j$  indicates the value of the  $j$ -th vehicle feature at the  $i$ -th time step.

The 3D geometry of the track will be used to extract a set of  $m \in \mathbb{N}$  road geometry features. We detail the choice of the vehicle and road geometry features in the next sections.

### A. Definition of the road geometry

In prediction and control applications, it is fundamental to describe the geometrical properties of environment with features characterised by a sufficiently smooth evolution over time. To model the road and the vehicle position along the track, we refer to the global coordinates of the left and right

road margins, the road centerline and the vehicle centre of gravity (CG) with respect to a global orthonormal reference frame  $X^G - Y^G - Z^G$ . The axis  $Z^G$  points in the opposite direction with respect to the gravity vector. We aim to derive parametric curves describing the margins and the centerline using 5<sup>th</sup>-order-polynomial splines, being the curvilinear abscissa the independent variable of each curve. Starting from the sampled global coordinates of the road margins, the splines knots are placed using piecewise linear interpolation and resampling with a coarser spacing. Then, the splines parameters are computed by minimising the splines normed distance from the original sampled points. The employment of 5<sup>th</sup>-order polynomials ensures the continuity of the splines up to the second derivative.

Keeping the centerline curvilinear abscissa as the independent variable and using the splines, it is possible to derive the following road geometry features:

- the road width;
- the first derivative of the coordinate in  $Z_G$  with respect to the centerline curvilinear abscissa, i.e. the pitch slope;
- the road bank angle, i.e. the lateral slope;
- the centerline signed curvature in the  $X^G - Y^G$  plane;
- the second derivative of the coordinate in  $Z_G$  with respect to the centerline curvilinear abscissa.

The values of these features carry information on the context in which the vehicle operates. The road width influences the lateral distance with respect to the centerline maintained by the driver along the track; the road pitch and lateral slopes play a key role in the dynamics of the vehicle, as they influence the orientation of the gravity vector with respect to the vehicle principal axes; finally, the centerline signed curvature in the  $X^G - Y^G$  plane and the second derivative of  $Z^G$  with respect to the centerline curvilinear abscissa provide information on the shape of the track, allowing to distinguish different types of turn and straightaway.

The global coordinates of the centerline are also employed as references to define the relative distance and relative yaw of the vehicle, which are included among the vehicle features, as described in the next section.

### B. Definition of the vehicle features

As specified above, the  $q$  vehicle features that we aim to forecast constitute a subset of the full set of  $n$  vehicle features considered in the method. The full set is fundamental to help the data-driven method learning the dynamics of the underlying physical process that we want to describe. Moreover, this becomes even more important considering that the driver could potentially lead the vehicle to very different situations on the track, so that a data-driven algorithm failing to understand the driver-vehicle system dynamics would not be able to correctly generalise on new data. In view of these considerations, we will show in Sec. III that the proposed data-driven scheme is designed to predict all of the  $n$  features, while it adopts a weighting strategy to maximise the prediction performance on the  $q$  desired features.

The selected  $n$  vehicle features are:

- the vehicle CG accelerations with respect to its principal axes;
- the vehicle chassis angular velocities with respect to its principal axes;
- the vehicle CG relative distance and vehicle chassis relative yaw with respect to the centerline;
- the vehicle CG velocities with respect to its principal axes;
- the throttle percentage, brake percentage, steering angle, steering angle rate and gear, i.e. driver commands.

In this case, the number of vehicle features is  $n = 16$ . It is necessary to notice that the choice of the vehicle features depends on the level of detail in the description of the vehicle dynamics that one is interested to model. In this work, we decide to model the part of the driver-vehicle system dynamics constituted by those features that can be measured/estimated and used for common control applications, e.g. ADAS. However, the framework is designed to be general, so that the user can include other features of interest into the problem.

### III. PROPOSED PREDICTION STRATEGY

The proposed prediction strategy is detailed in this section. The matrix  $X_{(k-t^P:k)}$ , introduced in Sec. II, will be referred to as matrix of the past from now on. It contains the information on the recent past that the system driver-vehicle has just experienced. As stated above, the past is not sufficient to fully characterise the behaviour of the system in the future, since it is highly correlated with the geometrical context that is encountered. To introduce the information on the road geometry that the driver sees ahead, we consider the curvilinear abscissa  $s_k$  of point  $P_k$ , defined as the point of the centerline that is closest to the vehicle CG at the time step  $k$ . Considering that at the current time step the road geometry influencing the finite horizon prediction depends on a limited portion of the whole track, we define the maximum distance that the driver can see ahead  $d^R \in \mathbb{R}$ ,  $d^R \geq 0$ , and the number of spatially equidistant discretisation points  $p^R \in \mathbb{N}$  in the continuous interval  $(s_k, s_k + d^R]$ . From the corresponding values of curvilinear abscissa, denoted as  $s_{k|1}, s_{k|2}, \dots, s_{k|p^R}$ , the road geometry features are evaluated and stored into matrix  $\bar{X}_k^R$ . Therefore, its structure is

$$\bar{X}_k^R := \begin{bmatrix} x_{k|1}^1 & x_{k|1}^2 & \dots & x_{k|1}^m \\ x_{k|2}^1 & x_{k|2}^2 & \dots & x_{k|2}^m \\ \dots & \dots & \dots & \dots \\ x_{k|p^R}^1 & x_{k|p^R}^2 & \dots & x_{k|p^R}^m \end{bmatrix}, \quad (2)$$

where  $x_{k|i}^j$  indicates the value of the  $j$ -th road feature evaluated at the curvilinear abscissa  $s_{k|i}$ .

Finally, following the considerations introduced in Sec. II-B, we introduce matrix  $\bar{X}_{(k+1:k+t^F)}$  expressing the full set of  $n$  vehicle features in the future  $t^F$  time steps, as

$$\bar{X}_{(k+1:k+t^F)} := \begin{bmatrix} x_{k+1}^1 & x_{k+1}^2 & \dots & x_{k+1}^n \\ x_{k+2}^1 & x_{k+2}^2 & \dots & x_{k+2}^n \\ \dots & \dots & \dots & \dots \\ x_{k+t^F}^1 & x_{k+t^F}^2 & \dots & x_{k+t^F}^n \end{bmatrix}. \quad (3)$$

We remark that matrix  $X_{(k+1:k+t^F)}$ , i.e. the goal of our problem, can be obtained by extracting the subset of  $q$  features of interest from matrix  $\bar{X}_{(k+1:k+t^F)}$ , being  $q \leq n$ .

#### A. Deep neural network

To solve the prediction problem formulated above, we propose a deep-learning architecture. The structure of the artificial neural network, exploiting an encoder-decoder topology to synthesize the information of the past  $X_{(k-t^P:k)}$  and the road seen ahead  $\bar{X}_k^R$ , is now presented.

The scheme of the network is shown in Fig. 1. The matrix of the past  $X_{(k-t^P:k)}$  is encoded using a bidirectional Long-Short-Term-Memory (LSTM) layer with  $u_e$  hidden units, for their high performance in sequence encoding [15]. The last hidden states  $h_F^P, h_B^P$ , and cell states  $c_F^P, c_B^P$  of the LSTM layers in the forward and backward directions are merged together through concatenation, to form one hidden states vector  $h^P$  and one cell states vector  $c^P$ . The road geometry matrix  $\bar{X}_k^R$  is encoded by means of another bidirectional LSTM layer with  $u_e$  hidden units, employing the same merge mechanism, to obtain the hidden states vector  $h^R$  and cell states vector  $c^R$ . The hidden states and cell states of the two encoders are then concatenated, to create an extended hidden states vector  $h$  and an extended cell states vector  $c$ . Two dense layers with  $2u_e$  and  $u_d$  neurons are applied to both  $h$  and  $c$  without weights sharing, to merge the information carried by the encodings of the past and the geometry of the road in the future, and to uniform them to the dimensions of the decoder. A dropout layer with rate  $r$  is placed between each couple of dense layers to promote regularisation. Consequently, the vectors  $h^D$  and  $c^D$  are generated.

The decoder consists of two stages. The first is a unidirectional LSTM layer with  $u_d$  hidden units, whose hidden and cell states are initialised using the vectors  $h^D$  and  $c^D$ . The first cell is fed with  $h^D$  as inputs. From the second cell on, the output of each LSTM cell is recursively used as input of the successive cell. The second stage of the decoder is a bidirectional LSTM layer of  $u_d$  hidden units, whose output sequences are fed to a final time-distributed dense layer, that brings the matrices to assume the output shape. The output of the network  $\hat{X}_{(k+1:k+t^F)}$  is the prediction of  $\bar{X}_{(k+1:k+t^F)}$ , which represents the ground truth. The entries of  $\hat{X}_{(k+1:k+t^F)}$  are denoted with  $\hat{x}_i^j$ , being it the value of the  $j$ -th vehicle feature at the  $i$ -th time step.

Finally, we define the two hyperparameters  $u_{e,d}$  and  $\xi$  as

$$u_{e,d} = u_e + u_d, \quad (4)$$

$$\xi = \frac{u_e}{u_{e,d}}. \quad (5)$$

These two hyperparameters synthetically express the total network complexity for the encoding and decoding parts. Since the total network complexity influences the computational time needed to generate a prediction, it is important to properly limit the values of  $u_{e,d}$  and  $\xi$  to render the proposed architecture feasible for online control applications. This consideration will be reminded in Sec. IV-B, where hyperparameters tuning is described.

#### B. Loss function

Taking advantage of how the problem is formulated in Sec. II, the proposed prediction framework is potentially able to forecast the values of any vehicle feature that one could be interested in. Independently from the specific subset of  $q$  features of interest for a determined application, it is important to design a loss function that penalises prediction errors on the full set of  $n$  vehicle features. This choice forces the network to learn the driver-vehicle system dynamics, and infuses a natural generalisation into the data-driven approach. The  $q$  features of interest and the remaining  $n - q$  ones are denominated as primary and secondary features, respectively.

To comply with the requirements of specific applications, in which one could be interested in maximising the prediction performance on the restricted set of  $q$  vehicle features, we employ Weighted Mean Square Error (WMSE) as loss function:

$$\mathcal{L} = \sum_{i=k+1}^{k+t^F} \frac{\sum_{j=1}^n w^j (\hat{x}_i^j - x_i^j)^2}{n}, \quad (6)$$

where  $w^j = 1$  for  $j = 1, \dots, q$  are the weights on the primary features, and  $w^j = w$  for  $j = q + 1, \dots, n$  are the weights on the secondary features. The hyperparameter  $w$  is in the range  $0 \leq w \leq 1$ , and is tuned depending on the application. The employment of the weighting term  $w$  is strictly related to the requirements of online applicability of the prediction strategy. In case online applicability were not an issue, the network complexity could be arbitrarily increased to predict all of the  $n$  vehicle features. Instead, in the case study of this work we aim to design a network with prediction times that are suitable for online control applications; thus, we use  $w$  to help the network identify the relative priority between the primary and secondary features.

### IV. APPLICATION TO A CASE STUDY

The proposed framework is validated by applying it to an interesting case study, namely the prediction of the features that are commonly fed as references to any modern motion cueing algorithm for dynamic driving simulators based on Model Predictive Control (MPC). Our code is available online<sup>1</sup>, whereas the corresponding dataset cannot be shared due to confidentiality reasons. We remark that the proposed methodology can also be employed to predict the evolution of any other feature that could be of interest for other automotive applications; we leave the study of further applications to future works.

Motion cueing is a planning algorithm that provides motion references to the dynamic platform of the simulator [16], [17]. The objective of the planning problem is to reproduce the translational accelerations and rotational velocities at the driver's head that would be generated on a real vehicle. In fact, it is through these quantities that humans perceive motion, thanks to their vestibular system. Modern implementations of motion cueing algorithms are based on constrained optimal control, to account for workspace limitations. The most used technique is MPC [18]–[20], whose formulation

<sup>1</sup>[https://github.com/lpapasusso/DLfmwk\\_driver](https://github.com/lpapasusso/DLfmwk_driver)



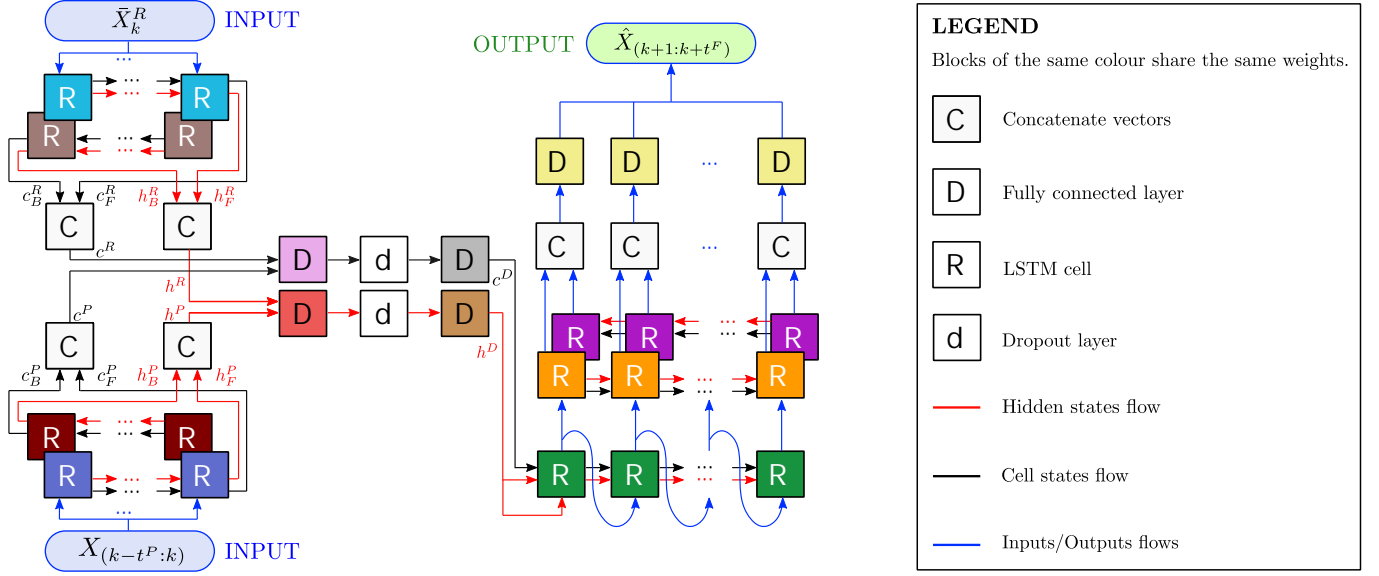


Fig. 1. Proposed deep neural network.

includes the system and reference evolution in the future (predictive horizon) to generate an optimised and prompt motion, anticipating future situations. However, the state-of-the-art solutions developed so far do not fully exploit the potential benefits introduced by MPC. To avoid predicting the future behaviour of the driver, they employ a constant reference throughout the predictive horizon, equal to the one that is measured in simulation at the time of execution. As shown in [21], knowing the reference future evolution in advance and extending the predictive horizon would allow to outperform the state-of-the-art results. For this reason, we will focus the attention of our network to prioritise the reconstruction of the vehicle CG longitudinal and lateral accelerations ( $a_X$  and  $a_Y$ , respectively), and vehicle chassis yaw rate ( $\omega_y$ ), being the in-plane motion the most crucial to enhance the simulator workspace utilisation. This means that the number of primary features is  $q = 3$ .

The performance of the prediction framework is tested for two different prediction horizon lengths, namely  $t^F = 30$  (i.e. 3 s) and  $t^F = 50$  (i.e. 5 s). In the first case, considering the maximum speed of the vehicle, we estimate that a suitable choice for the parameters that model the road geometry in the future is  $d^R = 150$  m and  $p^R = 50$ . In the second case, the prediction steps are increased to  $t^F = 50$  (5 s). Taking into account the longer prediction horizon,  $d^R = 250$  m and  $p^R = 83$  are selected.

#### A. Dataset preparation

The dataset used to validate the prediction framework was generated on a dynamic driving simulator, shown in Fig. 2. The simulation environment set up for our analysis is the Canadian test track Calabogie, whose planimetry is shown in Fig. 3. We collected a dataset of 36 laps performed by a non-professional driver, for a total of approximately 75 minutes and 160 km travelled. A non-professional human driver was selected for the tests to introduce high variability into the resulting motion

trajectories, which makes the prediction problem particularly challenging. The low level of repeatability of the driver at each lap is used to test the generalisation capability of the network. The latter is in fact expected to generate predictions that are close to the ground truth when the driving behaviour is more repeatable, and stabilise around an average behaviour when it is not.

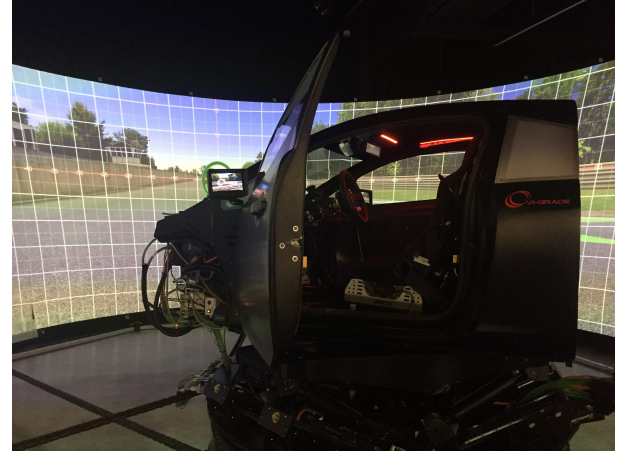


Fig. 2. Dynamic driving simulator used to collect the dataset.

The original data were acquired at a sampling frequency of 100 Hz. To be able to consider long-enough prediction horizons while saving the neural network computational time, data are downsampled at a frequency of 10 Hz, after using a zero-phase anti-aliasing filter with cut-off frequency at 4 Hz. As an example, Fig. 4 shows the original and downsampled frequency content of  $a_X$ ,  $a_Y$  and  $\omega_y$ . The downsampled signals contain approximately 98% of the power of the original ones; thus, the downsampling architecture allows to obtain a good trade-off between the level of detail in the representation of the driver-vehicle system dynamics and the speed of the

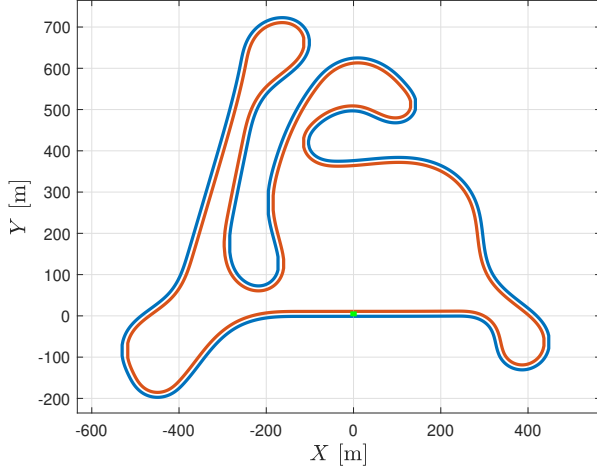


Fig. 3. Planimetry of the test track Calabogie used for the validation of the proposed approach. The right and left margins are shown in red and blue, respectively, i.e. the lap is clockwise. The start line is marked in green.

prediction algorithm, in terms of online computational time in the test phase. Lastly, the signals are normalised to facilitate the neural network training process.

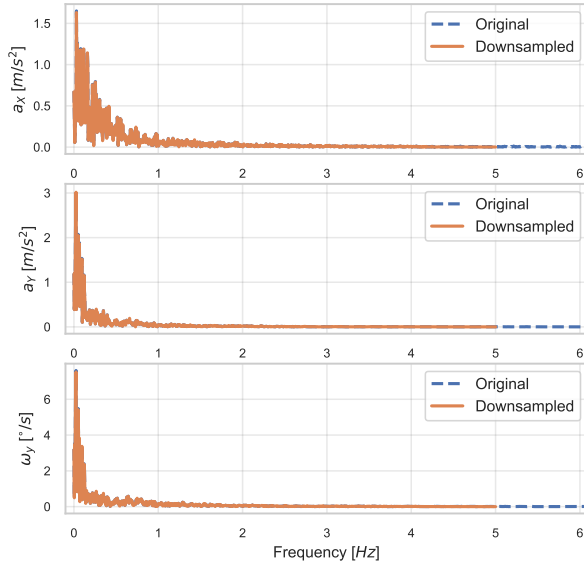


Fig. 4. Frequency content of the longitudinal acceleration  $a_X$ , lateral acceleration  $a_Y$  and yaw rate  $\omega_Y$ , for the original and downsampled signals. The downsampled signals contain approximately 98% of the power of the original ones.

### B. Training and validation of the model

The matrices defined in (1) are obtained by windowing each lap of the original dataset, using unitary shift and stride. A 31 – 4 – 1 random split of the laps is applied to obtain the training, validation and test sets, respectively.

The model is trained using the Adam optimiser [22], with  $\beta_1 = 0.9$ ,  $\beta_2 = 0.999$  and  $\epsilon = 10^{-7}$ . After a first coarse tuning, it was observed that the hyperparameters affecting the network performance are the dropout rate  $r$ , the weight

$w$  on the secondary features, the number of time steps of the past  $t^P$ , and the parameters  $u_{e,d}$  and  $\xi$  describing the structure of the network. To fine tune the parameters, we employ Bayesian optimisation [23] (using the toolbox [24]), which targets finding the best value of the metrics  $\mathcal{M}$  on the validation set. The metrics  $\mathcal{M}$  is the Mean Absolute Error (MAE) referred to the primary features only, i.e.  $a_X$ ,  $a_Y$  and  $\omega_Y$ :

$$\mathcal{M} = \sum_{i=k+1}^{k+t^F} \frac{\sum_{j=1}^q |\hat{x}_i^j - x_i^j|}{q}, \quad (7)$$

being  $|\cdot|$  the absolute value operator. The range of variation of each hyperparameter in Bayesian optimisation is reported in Table I. We highlight that the ranges of the hyperparameters  $u_{e,d}$  and  $\xi$  are properly set to reduce the complexity of the neural network, thus allowing to use the prediction approach in online control applications. Bayesian optimisation implements 2 steps of random exploration and 10 iterations.

TABLE I  
LIMITS OF THE HYPERPARAMETERS IN BAYESIAN OPTIMISATION.

Hyperparameters	min	max
$r$	0.25	0.5
$w$	0.0	1.0
$t^P$	15	40
$u_{e,d}$	70	110
$\xi$	0.3	0.5

The training process of each model generated by Bayesian optimisation is performed in two phases. In the first phase, the Adam optimiser starts from a random initialisation of the weights of the neural network; to re-initialise the optimizer with weights that are closer to the optimal ones, which favours a more precise gradient descent, the second phase starts from the final configuration of the first phase. We now detail the characteristics of the two training phases. The first phase implements an exponentially decaying learning rate, going from 0.001 to 0.0005 in 34 epochs; after epoch 34, the learning rate is kept constant. We set the maximum number of epochs to 100, while using an early stopping option that activates when the validation metrics does not decrease within 25 consecutive epochs. The second phase employs a constant learning rate equal to 0.0001, with the same early stopping option as the first phase and a maximum number of epochs equal to 500. A batch size equal to 64 showed the best performance.

### C. Analysis of the results

In this section, the results of the case study are presented and analysed. The optimal hyperparameters configuration resulting from Bayesian optimisation is reported in Table II. It is interesting to notice that the optimal number of neurons of the encoders  $u_e$  is equal to 32 in both the cases. Also, the optimal number of steps in the past is  $t^P = 21$  and  $t^P = 30$  for the two prediction horizon lengths, respectively. This highlights that it is sufficient to observe approximately 2 – 3 s of the past

to characterise the current driving condition/situation, which is likely for the dynamics of the driver-vehicle system.

TABLE II  
OPTIMAL CONFIGURATION OF THE HYPERPARAMETERS RESULTING FROM BAYESIAN OPTIMISATION.

Hyperparameters	$t^F = 30$	$t^F = 50$
$r$	0.4116	0.3246
$w$	0.3138	0.7385
$t^P$	21	30
$u_{e,d}$	80	94
$\xi$	0.4000	0.3404

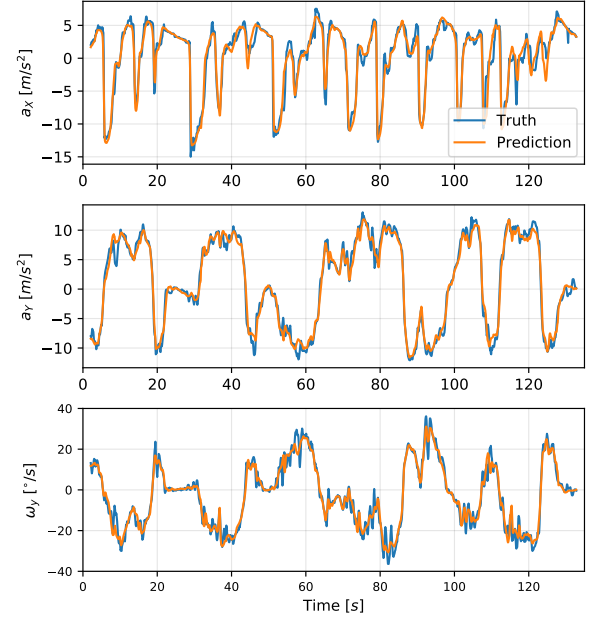
Considering the high variability of motion of the non-professional driver and the relatively small size of the dataset, we perform cross-validation to obtain performance indices that do not depend on the specific data split. Therefore, fixing the optimal hyperparameters obtained through Bayesian optimisation, training is finally repeated 10 times, changing the training, validation and test sets at each iteration. The statistics of the loss and metrics for the 10 iterations is reported in Table III. We remark that, since (6) and (7) refer to a single window of prediction, the loss/metrics over the full sets is obtained by summing together each loss/metrics and dividing by the total number of windows.

The prediction of the variables of interest, i.e.  $a_x$ ,  $a_y$  and  $\omega_y$ , along the test lap is reported in Fig. 5 for the two prediction horizons. Despite the highly variable behaviour of the non-professional driver, the proposed prediction framework succeeds in distinguishing the different portions of the road and generates context-aware predictions. As expected, the forecasting performance is higher in the points of the track where the driver behaviour is more repeatable. Instead, the network filters out the fast oscillations that derive from sporadic actions, stabilising around an average value that still properly captures the dominant trend of the dynamics. To better visualise the forecasting performance in a whole prediction window, we report two examples for each of the two prediction horizon lengths in Fig. 6.

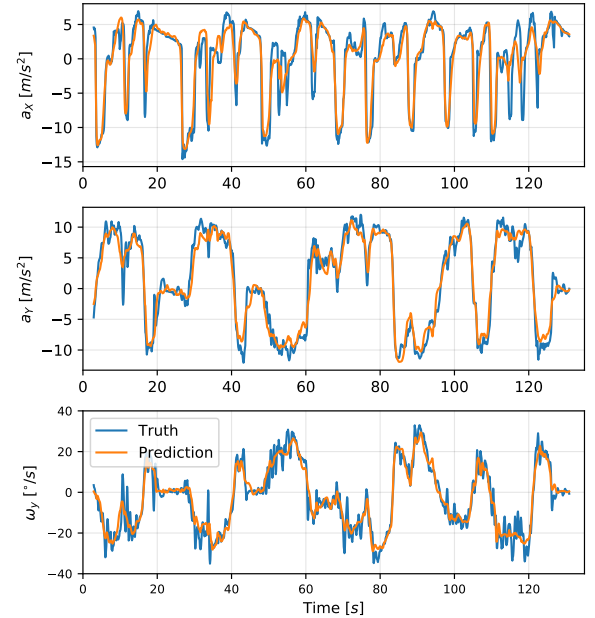
Finally, we evaluate the computational time of the neural network in the test phase. The results obtained for 40 consecutive windows are shown in Fig. 7. Considering the neural network trained for  $t^F = 30$ , the average computational time of a prediction window is 32 ms, with a sample standard deviation of 2 ms. For the  $t^F = 50$  case, the average computational time is 35 ms, with a sample standard deviation of 2 ms. The tests were run using interpreted Python code on a PC with an Intel Core i7-8565U CPU and 16 GB RAM. The measured computational times are already suitable for online control applications; however, we remark that it may be possible to further increase performance by resorting to compiled code and executing the operations on dedicated GPUs.

## V. GENERALISATION ON NEW DRIVERS AND TRACKS

As a last test to check its generalisation properties, the trained neural network with  $t^F = 30$  is used to predict state



(a) Case with  $t^F = 30$ .



(b) Case with  $t^F = 50$ .

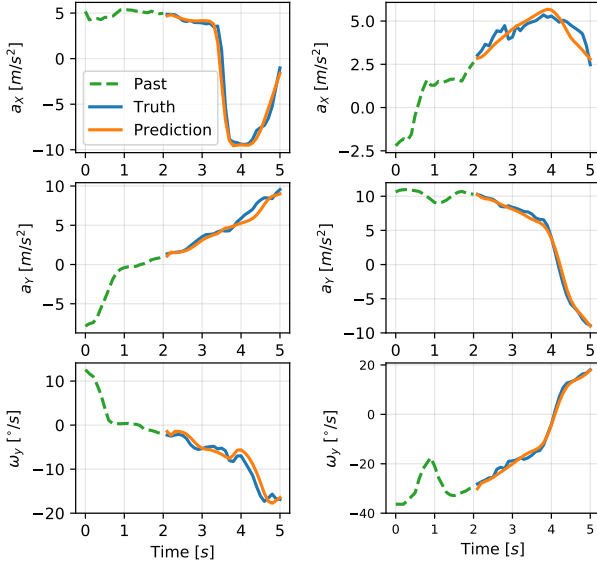
Fig. 5. Prediction of the variables of interest along the test lap. Each point of the orange curves represents the value predicted 30 (a) and 50 (b) time steps earlier.

trajectories from a new dataset, generated under considerably different high-level conditions with respect to the one employed for training and validation. In particular, we evaluate the prediction performance of the network by changing driver and track, respectively, in two separated tests.

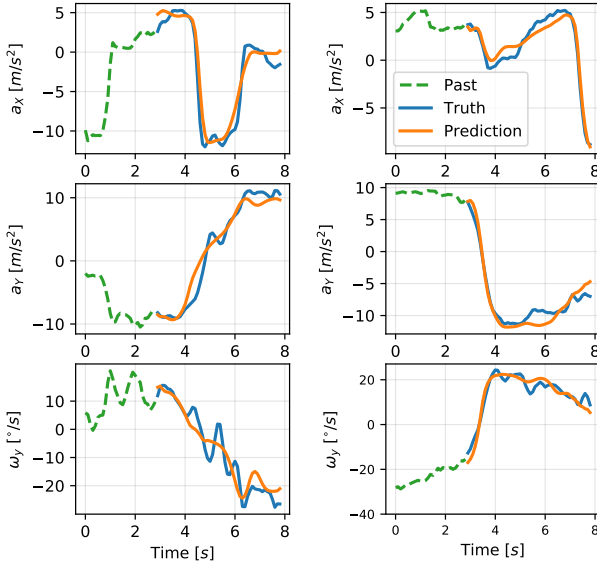
It is necessary to point out that this last analysis is not expected to show particularly high prediction performance. This is in line with the fact that we employed training and validation sets whose degree of variability is referred to the stochastic behaviour of the specific driver as a function of the

TABLE III  
SAMPLE AVERAGE  $\mu$  AND STANDARD DEVIATION  $\sigma$  OF THE LOSS AND METRICS USING CROSS-VALIDATION. THE VALUES ARE REFERRED TO THE NORMALISED DATA.

Sets	$t^F = 30$				$t^F = 50$			
	Loss		Metrics		Loss		Metrics	
	$\mu$	$\sigma$	$\mu$	$\sigma$	$\mu$	$\sigma$	$\mu$	$\sigma$
Training	0.0212	0.0006	0.1246	0.0025	0.0979	0.0058	0.1475	0.0057
Validation	0.0314	0.0019	0.1582	0.0061	0.1321	0.0083	0.1763	0.0065

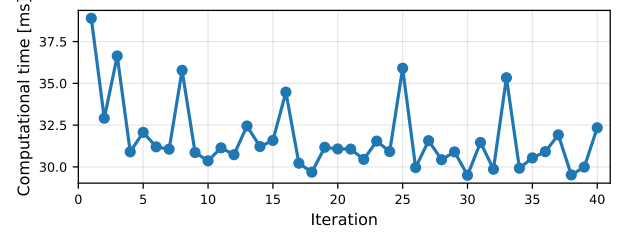


(a) Case with  $t^F = 30$ .

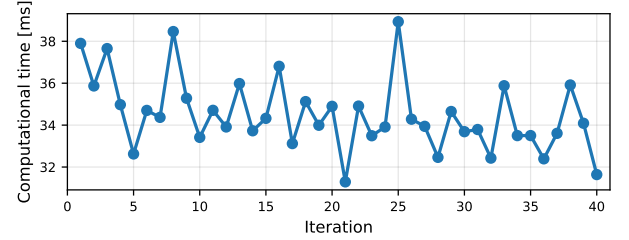


(b) Case with  $t^F = 50$ .

Fig. 6. Two prediction windows (left and right) extracted from the test lap for the two prediction horizons.



(a) Case with  $t^F = 30$ .



(b) Case with  $t^F = 50$ .

Fig. 7. Computational time of the neural network for 40 consecutive windows in the test phase.

variety of geometries in a given track, and not to different high-level scenarios, i.e. different drivers and tracks. Rather, this last analysis is meant to assess how far the current training/validation set is from an ideal one whose range of variability allows to achieve high prediction performance on a generic high-level scenario.

Considering the case of a test lap performed by a different driver, the prediction performance is shown in Fig. 8. The long-term predictions for  $a_Y$  and  $\omega_y$  properly follow the main trend of the ground truth, whereas the performance on  $a_X$  has significantly decreased. Since  $a_X$  is highly correlated with the throttle and brake percentages executed by the driver, this suggests that the new driver has different reaction times and aggressiveness with respect to the original driver. To cope with these aspects, future works will explore different techniques that may help the network to adapt to different types of driver. An interesting solution may be to use transfer learning [25] to adapt the pre-trained neural network to the style of a new driver. Alternatively, a clustering algorithm may be employed to distinguish driving styles and provide additional information to the neural network.

Finally, the results obtained by changing the track are reported in Fig. 9. The new track is obtained by travelling



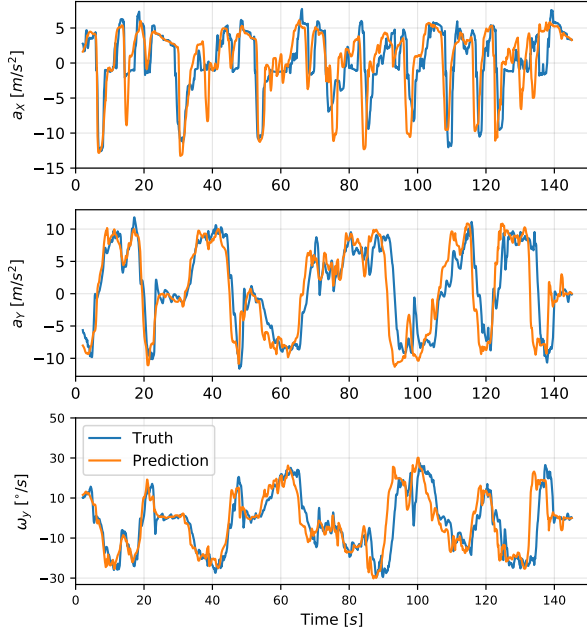


Fig. 8. Prediction of the variables of interest for the  $t^F = 30$  case, using a test lap performed by a different driver. Each point of the orange curves represents the value predicted 30 time steps earlier.

the original test track in opposite direction. For completeness, it has to be remarked that a track travelled in opposite direction generates driver-vehicle dynamics that are totally different and independent from the ones experienced in the original direction. Despite the neural network was trained on a single track, exploring few of the possible combinations of road geometry, it manages to reconstruct the main trend of  $a_y$  and  $\omega_y$  on the new track. This confirms that the proposed architecture succeeds in linking the decisions of the driver with the geometry of the road. Thus, by selecting a suitable set of tracks to populate the dataset, it may be possible to optimise the generalisation capabilities of the network, making it robust to new tracks. This analysis is left to future works.

## VI. CONCLUSIONS

This paper presented a deep-learning framework to predict state trajectories of a human-driven vehicle, travelling on a track with complex geometry. It is based on a flexible problem formulation, so that the user can choose a generic set of signals to be forecast. To show a practical implementation of the algorithm, a predefined set of features useful for control applications was selected. One of the innovative contributions of this work is the inclusion of the road geometry into the prediction algorithm, to link the actions executed by the driver to the shape of the road that he/she travels. The prediction problem is solved with a deep neural network, whose complexity is constrained to allow for use in online control applications. The computational times obtained during tests confirmed the suitability of the method.

The efficacy of the proposed approach was validated in an interesting case study regarding motion cueing algorithms, with the corresponding dataset being generated in test sessions

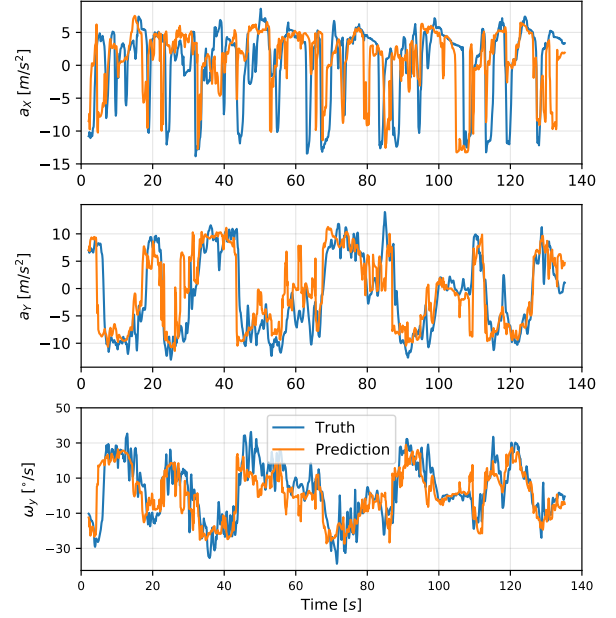


Fig. 9. Prediction of the variables of interest for the  $t^F = 30$  case, using a test lap performed on a different track. Each point of the orange curves represents the value predicted 30 time steps earlier.

of a non-professional human driver on a dynamic driving simulator. The scheme showed good performance in predicting the desired signals, namely the longitudinal and lateral accelerations of the vehicle, and its yaw rate.

Finally, the generalisation capabilities of the trained neural network on two new test sets, generated by changing driver and track, respectively, were analysed and commented. Despite the new test sets were out of the scope of the training/validation sets, the neural network managed to forecast the main trends of the lateral acceleration and yaw rate. This demonstrated the effectiveness of the approach in linking the future predictions with the past dynamics of the driver-vehicle system and the road geometry. Future works shall define a minimal set of drivers and tracks to possibly improve the generalisation capabilities of the neural network on any new driver/track configuration. Also, the design of methods to enhance an automatic adaptation of the network to different drivers and tracks will be investigated.

## REFERENCES

- [1] J. Kutz, "Deep learning in fluid dynamics," *Journal of Fluid Mechanics*, vol. 814, pp. 1–4, Mar. 2017.
- [2] E. Yeung, S. Kundu, and N. Hodas, "Learning Deep Neural Network Representations for Koopman Operators of Nonlinear Dynamical Systems," in *2019 American Control Conference (ACC)*, Jul. 2019, pp. 4832–4839.
- [3] J. Morton, T. A. Wheeler, and M. J. Kochenderfer, "Analysis of recurrent neural networks for probabilistic modeling of driver behavior," *IEEE Transactions on Intelligent Transportation Systems*, vol. 18, no. 5, pp. 1289–1298, May 2017.
- [4] A. Zyner, S. Worrall, and E. Nebot, "Naturalistic Driver Intention and Path Prediction Using Recurrent Neural Networks," *IEEE Transactions on Intelligent Transportation Systems*, vol. 21, no. 4, Apr. 2020.
- [5] P. Wang, H. Liu, L. Wang, and R. Gao, "Deep learning-based human motion recognition for predictive context-aware human-robot collaboration," *CIRP Annals - Manufacturing Technology*, vol. 67, pp. 17–20, Jul. 2018.

- [6] J. Zhang, H. Liu, Q. Chang, L. Wang, and R. Gao, "Recurrent neural network for motion trajectory prediction in human-robot collaborative assembly," *CIRP Annals - Manufacturing Technology*, vol. 69, pp. 9–12, Jul. 2020.
- [7] A. Dominguez-Sanchez, M. Cazorla, and S. Orts-Escolano, "Pedestrian movement direction recognition using convolutional neural networks," *IEEE Transactions on Intelligent Transportation Systems*, vol. 18, no. 12, pp. 3540–3548, Dec. 2017.
- [8] B. Ivanovic, A. Elhafi, G. Rosman, A. Gaidon, and M. Pavone, *MATS: An Interpretable Trajectory Forecasting Representation for Planning and Control*, Sep. 2020.
- [9] C. Cacciabue, *Modelling Driver Behaviour in Automotive Environments: Critical Issues in Driver Interactions with Intelligent Transport Systems*. London: Springer-Verlag, 2007.
- [10] M. Plöchl and J. Edelmann, "Driver models in automobile dynamics application," *Vehicle System Dynamics*, vol. 45, no. 7-8, pp. 699–741, Jul. 2007.
- [11] T. D. Gillespie, *Fundamentals of Vehicle Dynamics*. Warrendale: SAE International, 1992.
- [12] W. F. Milliken and D. L. Milliken, *Race Car Vehicle Dynamics*. Warrendale: SAE International, 1994.
- [13] M. Blundell and D. Harty, *The Multibody Systems Approach to Vehicle Dynamics*. Oxford: Elsevier, 2004.
- [14] F. Braghin, F. Cheli, S. Melzi, and E. Sabbioni, "Race driver model," *Computers & Structures*, vol. 86, no. 13, pp. 1503–1516, Jul. 2008.
- [15] D. Britz, A. Goldie, M.-T. Luong, and Q. Le, "Massive exploration of neural machine translation architectures," in *Proceedings of the 2017 Conference on Empirical Methods in Natural Language Processing*, Jan. 2017, pp. 1442–1451.
- [16] H. Asadi, S. Mohamed, C. P. Lim, and S. Nahavandi, "Robust optimal motion cueing algorithm based on the linear quadratic regulator method and a genetic algorithm," *IEEE Transactions on Systems, Man, and Cybernetics: Systems*, vol. 47, no. 2, pp. 238–254, Feb. 2017.
- [17] A. Mohammadi, H. Asadi, S. Mohamed, K. Nelson, and S. Nahavandi, "Multiobjective and Interactive Genetic Algorithms for Weight Tuning of a Model Predictive Control-Based Motion Cueing Algorithm," *IEEE Transactions on Cybernetics*, vol. 49, no. 9, pp. 3471–3481, Sep. 2019.
- [18] A. Beghi, M. Bruschetta, and F. Maran, "A real time implementation of MPC based Motion Cueing strategy for driving simulators," in *2012 IEEE 51st IEEE Conference on Decision and Control (CDC)*, Dec. 2012, pp. 6340–6345.
- [19] —, "A Real-Time Implementation of an MPC-Based Motion Cueing Strategy with Time-Varying Prediction," in *2013 IEEE International Conference on Systems, Man, and Cybernetics*, Oct. 2013, pp. 4149–4154.
- [20] M. Bruschetta, C. Cenedese, and A. Beghi, "A real-time, MPC-based Motion Cueing Algorithm with Look-Ahead and driver characterization," *Transportation Research Part F: Traffic Psychology and Behaviour*, vol. 61, pp. 38–52, Feb. 2019.
- [21] M. Grottoli, D. Cleij, P. Pretto, Y. Lemmens, R. Happee, and H. Bühlhoff, "Objective evaluation of prediction strategies for optimization-based motion cueing," *SIMULATION: Transactions of The Society for Modeling and Simulation International*, vol. 95, Dec. 2018.
- [22] D. Kingma and J. Ba, "Adam: A method for stochastic optimization," *3rd International Conference on Learning Representations (ICLR)*, May 2015.
- [23] M. Pelikan and D. E. Goldberg, "BOA: The Bayesian optimization algorithm," in *GECCO'99: Proceedings of the 1st Annual Conference on Genetic and Evolutionary Computation*, vol. 1, Jul. 1999, pp. 525–532.
- [24] F. Nogueira, "Bayesian Optimization: Open source constrained global optimization tool for Python," 2014–. [Online]. Available: <https://github.com/fmfn/BayesianOptimization>
- [25] C. Tan, F. Sun, T. Kong, W. Zhang, C. Yang, and C. Liu, "A Survey on Deep Transfer Learning," in *Artificial Neural Networks and Machine Learning – ICANN 2018*, ser. Lecture Notes in Computer Science, vol. 11141, Oct. 2018, pp. 270–279.



**Luca Paparusso** received the M.Sc. degree in mechanical engineering from Politecnico di Milano, Italy, in 2018, where he is pursuing the Ph.D. degree. He was research fellow at Istituto Italiano di Tecnologia (IIT), Italy, in 2019. His research is focused on motion prediction to improve automated systems control.



**Stefano Melzi** received the M.Sc. degree in mechanical engineering in 1999 and the Ph.D. in applied mechanics in 2003 from Politecnico di Milano, Italy, where he is associate Professor since 2014. His research activity deals in general with dynamics of mechanical systems and, in particular, on the dynamics of ground vehicles and interaction of wind with overhead transmission lines. He is author of nearly 150 publications almost entirely at international level.



**Francesco Braghin** received the M.Sc. degree in mechanical engineering in 1997 and Ph.D. in applied mechanics in 2001 from Politecnico di Milano, Italy, where he is full Professor since 2015. Author of more than 250 scientific publications, his research is carried out in the field of vehicle dynamics (road and railway) and mechatronics. In particular, as regards road vehicles, his research deals with the modelling of tires and their interaction with the soil, and the application of optimal control algorithms to the design of hybrid and electric vehicles, as well as to the development of fully autonomous vehicles.